Proceedings Paper:

Lei, H., Chong, B. orcid.org/0000-0001-5977-7197 and Li, K. MPC Based Optimal Energy Management of Electrical Vehicles with Hybrid Energy Storage on Fixed Routine. In: UNSPECIFIED IEEE Transportation Electrification Conference and Expo + Electric Aircraft Technologies Symposium, 18-20 Jun 2025, Anaheim, California. IEEE (In Press)

MPC Based Optimal Energy Management of Electrical Vehicles with Hybrid Energy Storage on Fixed Routine

Hanlin Lei
School of Electronic and Electrical Engineering
University of Leeds
Leeds, Unite Kingdom
Email: elhle@leeds.ac.uk

Benjamin Chong
School of Electronic and Electrical Engineering
University of Leeds
Leeds, Unite Kingdom
Email: B.Chong@leeds.ac.uk

Kang Li
School of Electronic and Electrical Engineering
University of Leeds
Leeds, Unite Kingdom
Email: K.Li1@leeds.ac.uk

***Abstract*—This article presents a model predictive control (MPC) based energy management strategy for electric vehicles powered by hybrid power sources, focusing on their performance improvements while running on fixed routines. The idea is to utilize the historic operation data to improve the energy allocation optimization solutions, with the goal of enhancing the energy efficiency of electric vehicles running on fixed driving routes by minimising losses through minimum battery current operations and extending the vehicles' driving range. Key contributions include the formulation of a model predictive control based energy allocation problem, and the implementation of convex hull constrained MPC based on historic data. Simulation results demonstrate the continual performance improvements in the presence of uncertainties being introduced into the system.**

I. Introduction

In the field of electric vehicle research, heavy-duty electric vehicles is receiving more and more attention compared to small vehicles. This is because small electric vehicles with single energy storage systems are currently highly matured in technology. Moreover, for heavy-duty electric vehicles and high-performance electric sports cars, larger and more diverse energy storage systems can be utilized to provide greater energy output[1].

The hybrid energy storage system consisting of batteries and supercapacitors is often seen in electric vehicle applications[2]. Battery are typically used as a main energy system with high energy storage capacity, and supercapitor is used as an auxiliary energy system with high power capability and reversibility[3].

Popular energy management approaches for hybrid energy electric vehicles include rule-based control, filtering control, fuzzy logic control, model predictive control, etc[4]. Due to the existence of unmodeled dynamics, sensor noise or measurement errors, component limitations or failures, and other uncertainties and disturbances, these energy management approaches may not be as effective as claimed[5].

For application scenarios where electric vehicles run on fixed routines, such as buses and logistic fleets, model predictive control offers a desirable framework where the cost functions, constraints, and system model can be modified and updated, thereby offering continual performance improvement potentials[6].

This article designs an electric vehicle energy management system based on model predictive control, suitable for electric vehicle driving on fixed routine.. The convex hull of historical data is used as a constraint for model predictive control.

II. Energy Management System Design

A. System Diagrams

The system diagram of the system is shown in Fig. 1. The goal of this system design is to optimize the energy efficiency of electric vehicles (EVs) that operate on repetitive routes. This is achieved by minimizing the current drawn from the battery while stabilizing the supercapacitor's voltage at a reference value.

The vehicle's model receives speed and acceleration data to compute the total power demand, which is sent to the high-level MPC based planner, which is the focus of this paper. The high level MPC planner provides reference signals (battery current I_B and supercapacitor voltage V_{SC}) to the low-level controller, which generates control signals.

Measurements from the hybrid energy storage system (I_B and V_{SC}) are sent back to the low-level controller to the low-level controller to form a closed-loop control system. The latter is for energy management and operations control for the power electronic circuit used in the hybrid energy storage system.

B. Vehicle's Model

The vehicle is regared as a rigid body, so the longitudinal dynamics of a vehicle that includes the various forces acting on it during motion is considered. The longitudinal vehicle modeling power balance equation is given as equation (1), which is from [7].

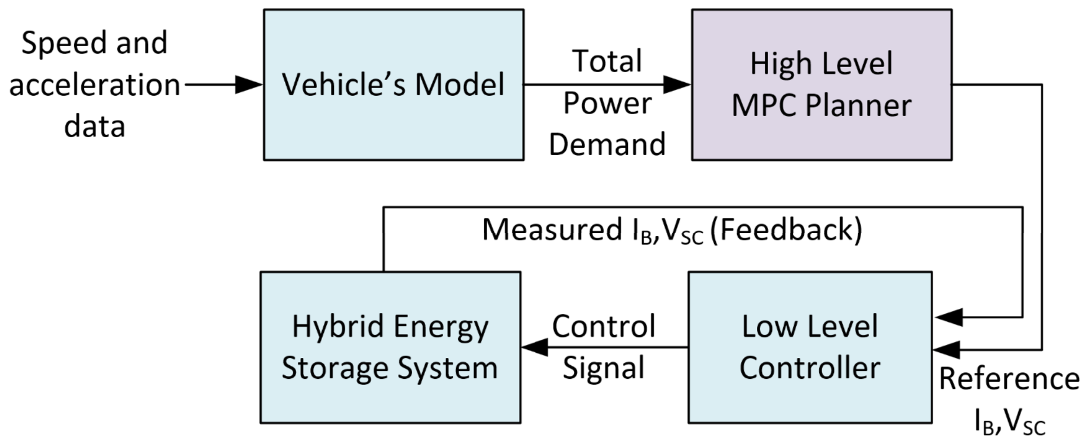

Fig. 1. System Diagram

$$P_\mathrm{e}=\frac{1}{1000}\cdot\frac{1}{\eta_\mathrm{T}}\left(\frac{mgfu_\mathrm{a}}{3.6}+\frac{mgu_\mathrm{a}\tan\alpha}{3.6}\right.$$
$$\left.+\frac{1}{2}\cdot\frac{C_\mathrm{D}A\rho u_\mathrm{a}^3}{3.6^3}+\frac{\delta m u_\mathrm{a}}{3.6}\cdot\frac{\mathrm{d}u_a}{\mathrm{d}t}\right) \quad (1)$$

In this equation, P_e is the power demand for every time step, the unit of P_e is kw. u_a is the vehicle speed in km/h, m is the vehicle's loaded mass in kg, f is the rolling resistance coefficient, g is the gravitational acceleration in m/s^2, ρ is the air density in kg/m^3, α is the road grade, C_D is the air resistance coefficient, g is the gravitational acceleration in m/s^2, A is the windward area of the vehicle in m^2, δ is the correction coefficient of the rotation mass, η_T is the efficiency of the transmission system.

The speed and acceleration data utilized in this system are based on the New York bus driving cycle because new york bus is a type of heavy duty vehicle.The data can be accessed from the U.S. Environmental Protection Agency official website[8] and also the Powertrain Blockset of MATLAB Simulink which is shown on Fig.2.

The speed and acceleration data from the driving cycle are fed into the power balance equation and then the total power demand at each time step can be calculated.

III. Model Predictive Control Formulation

A. Process Model

To effectively manage the energy exchange between these battery and supercapitor, mathematical models must capture their internal characteristics, such as the state of charge (SOC), power, internal resistance. These models provide the foundation for simulating the system's behaviour under different operating conditions and form the basis for control system design. The nonlinear equations for the battery and supercapacitor are shown as equation(2) and (3), which is from[9]:

$$S\dot{O}C_B=\frac{V_\mathrm{OC}-\sqrt{V_\mathrm{OC}^2-4R_BP_B}}{2R_BQ_B} \quad (2)$$

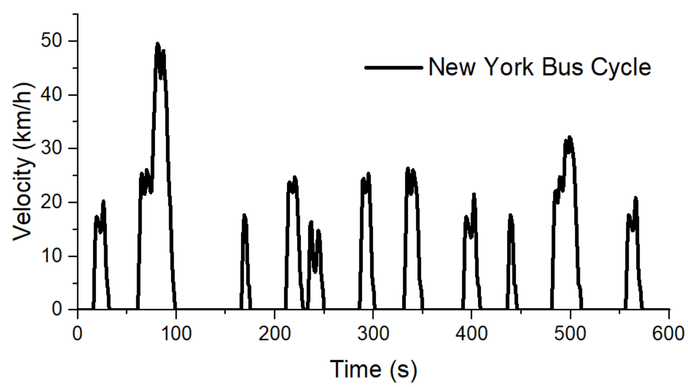

Fig. 2. NYBC Drive Cycle

$$S\dot{O}C_\mathrm{SC}=\frac{SOC_\mathrm{SC}V_\mathrm{max}-\sqrt{(SOC_\mathrm{SC}V_\mathrm{max})^2-4R_\mathrm{SC}P_\mathrm{SC}}}{2R_\mathrm{SC}C_\mathrm{SC}V_\mathrm{max}} \quad (3)$$

The linearization process is used to make the battery and supercapacitor model suitable for state-space equations. The linearized equations can be written in a standard matrix form as equation (4) and (5) given below, where K_1 and K_2 are constants, δ_1 and δ_2 are the system uncertainties:

$$\begin{bmatrix}\mathrm{SOC}_B(t+1)\\ \mathrm{SOC}_{sc}(t+1)\end{bmatrix}=\begin{bmatrix}A_B+\delta_1 & 0\\ 0 & A_{sc}+\delta_2\end{bmatrix}\begin{bmatrix}\mathrm{SOC}_B(t)\\ \mathrm{SOC}_{sc}(t)\end{bmatrix}$$
$$+\begin{bmatrix}B_B & 0\\ 0 & B_{SC}\end{bmatrix}\begin{bmatrix}P_B(t)\\ P_{sc}(t)\end{bmatrix}+\begin{bmatrix}K_1\\ K_2\end{bmatrix} \quad (4)$$

$$\begin{bmatrix}SOC_B(t)\\ V_{SC}(t)\end{bmatrix}=\begin{bmatrix}C_B & 0\\ 0 & C_{SC}\end{bmatrix}\begin{bmatrix}\mathrm{SOC}_B(t)\\ \mathrm{SOC}_{SC}(t)\end{bmatrix} \quad (5)$$

The input variables, state variables and output variables are

$$x(t)=\begin{bmatrix}SOC_B(t)\\ SOC_{SC}(t)\end{bmatrix},\quad u(t)=\begin{bmatrix}P_{BB}(t)\\ P_{SC}(t)\end{bmatrix},$$
$$y(t)=\begin{bmatrix}I_B(t)\\ V_{SC}(t)\end{bmatrix} \quad (6)$$

B. Cost function

The cost function consists primarily of three components: the square of the battery current, the rate of change of current, and the difference between the supercapacitor's operating voltage and its reference voltage[9]. The cost function is expressed by the following equation (7).

$$J=\min \sum_{i=1}^{P}\left[w_1\left(I_B(k+i \mid k)\right)^2+w_2\left(\frac{\mathrm{d} I_{\mathrm{bat}}(k+i \mid k)}{\mathrm{d} t}\right)^2 + w_3\left(V_{\mathrm{SC}}(k+i \mid k)-V_{\mathrm{SC}, \mathrm{ref}}\right)^2\right] \tag{7}$$

The values of w_1, w_2, w_3 are selected based on a trade-off between energy efficiency, battery health, and system stability according to[10]. The reference voltage for the supercapacitor is set to $0.75 V_{\mathrm{SC}, \mathrm{MAX}}$[9].

Since the supercapacitor's voltage is proportional to its SOC, this cost function can also be used to regulate the supercapacitor's SOC, ensuring system readiness to meet the power demands. Minimizing the current drawn from the battery reduces energy losses in the form of heat and reduces the load on the battery, thus extending its life[11].

C. Constraints

The SOC for both the battery and the supercapacitor must be maintained within predefined safe limits to avoid damage, ensure efficient operation, and extend the lifespan of the energy storage devices. They are defined as:

$$SoC_{B,\min} \leq \mathrm{SOC}_B \leq \mathrm{SOC}_{B,\text{ max}} \tag{8}$$

$$\mathrm{SOC}_{\mathrm{SC},\min} \leq \mathrm{SOC}_{\mathrm{SC}} \leq \mathrm{SOC}_{\mathrm{SC},\max} \tag{9}$$

The battery SOC ranges from 0.1 to 0.99 - such operating range is chosen for this research so that the investigation covers various conditions including those under extreme cases. For the supercapacitor, operating below 50% SOC reduces efficiency and increases internal resistance, which may affect its ability to provide rapid power response. To ensure both efficiency and fast response, its SOC is set between 0.5 and 0.99.

The power delivered by the battery and the supercapacitor are constrained to prevent overstressing either component. They are defined as:

$$P_{B,\text{ min}} \leq P_B \leq P_{B,\text{ max}} \tag{10}$$

$$P_{\mathrm{SC},\text{ min}} \leq P_{\mathrm{SC}} \leq P_{\mathrm{SC},\text{ max}} \tag{11}$$

$$P_B + P_{SC} = P_{demand} \tag{12}$$

The battery supplies up to 90% and the supercapacitor up to 60% of the maximum load power. The $P_{B,\text{ max}}$ and P_{SC} are calculated through that percentage. P_{demand} is already calculated through the previous process according to equation1. The maximum load demand is calculated based on driving cycle data and the vehicle model. This setting can avoid excessive use of a single energy source[2].

IV. Historical Data Handling Method

The control solutions of conventional MPC may not be the most effective, considering the uncertainties introduced into the system. This paper, therefore, addresses this and Fig. 3 and 4 illustrates the core of the algorithm used in this paper, which is to optimize the control input under the framework of model predictive control with the convex hull constraints based on the historic data and the strategy of variable priority positioning in the convex hull[12]. This convex hull defines a multidimensional space covering the actual possible states of the system, providing a feasible region for the optimization process.

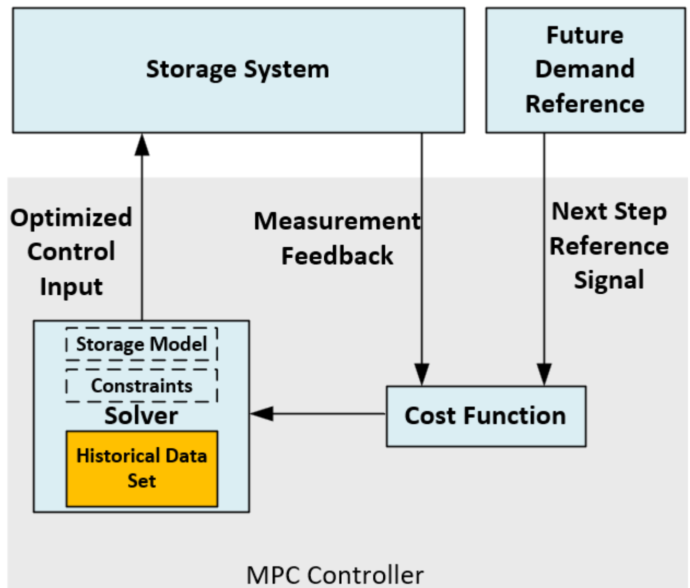

Fig. 3. Historical Data Handling in MPC Based Energy Storage Management

The yellow box part in Fig. 3 and 4 constitutes a core contribution of the algorithm applied in this paper. Equation (13) and its constraints are used to ensure that the predicted state remains within the convex hull formed by historical data. $\hat{\mathbf{x}}(t+p|t)$ denotes the prediction of the future state at time t. Each $\mathbf{x}_i$ corresponds to a known historical state, indexed by i, representing different sampling points.

$$\hat{\mathbf{x}}(t+p|t)=\sum_{i=0}^{t-1} \alpha_i \mathbf{x}_i+\mathbf{S} \quad (\mathbf{S} \geq 0) \tag{13}$$

The coefficient α_i denotes the weight assigned to each historical state in forming the predicted state $\hat{\mathbf{x}}(t+p|t)$ and α needs to meet the following requirements.

$$\sum_{i=1}^{t-1} \alpha_i=1 (\alpha_i \geq 0) \tag{14}$$

The non-negativity in equation (14) prevents any historical state from being assigned a negative weight, maintaining physical relevance in the prediction. The normalization constraint

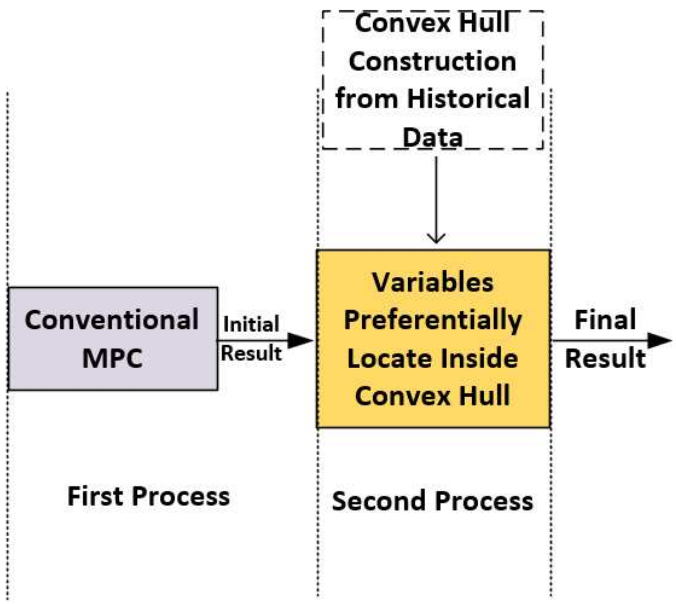

Fig. 4. Historical Data Handling Process

equation (14) forming $\hat{\mathbf{x}}(t+p|t)$ a convex combination of historical states.

In the simulation implementation, the convex hull is formed by solving the minimum polyhedron containing the historical data set and then the control solution is effectively confined to the convex hull area. The existence of the convex hull provides an adaptive feasibility guarantee for the controller, preventing the control solution from deviating from the actual working conditions during execution.

This paper also further introduces the optimization strategy of "variables are preferentially positioned inside the convex hull", but also introduces slack variables S, which allow the control solution to violate the constraints within a certain range to identify a more effective control effect. In complex load environments, this relaxation mechanism provides controllable fault tolerance, allowing the system to find a feasible solution with a smaller error when facing strict constraints or extreme working conditions.

V. Result and Analysis

In this section, the performance of battery current and supercapacitor voltage under different disturbance conditions and control iterations is analyzed to evaluate the effectiveness and convergence of the control algorithm in achieving energy management over multiple iterations. Figure 5 and Figure 6 shows the variation in battery current under ideal control(without disturbance), disturbance addition, and five iterations. The maximum voltage of the supercapacitor is 1400 V, so 75% of the maximum voltage will be 1050 V.

Under ideal scenario, battery current and supercapacitor voltage follow the desired trajectories smoothly optimized by conventional MPC with no disturbances. Then with the added disturbances, the system experiences significant fluctuations, especially in battery current peaks and supercapacitor voltage spikes, indicating that the disturbance had a large impact on the control system.

However, with the enabling of historical data handling control algorithm, as iterations proceed, these deviations is effectively mitigated from their ideal control scenarios, with both battery current and voltage closely approaching the ideal control solutions. This shows that the control strategy successfully suppressed the fluctuations caused by the disturbance in multiple iterations, demonstrating improved adaptability and stability.

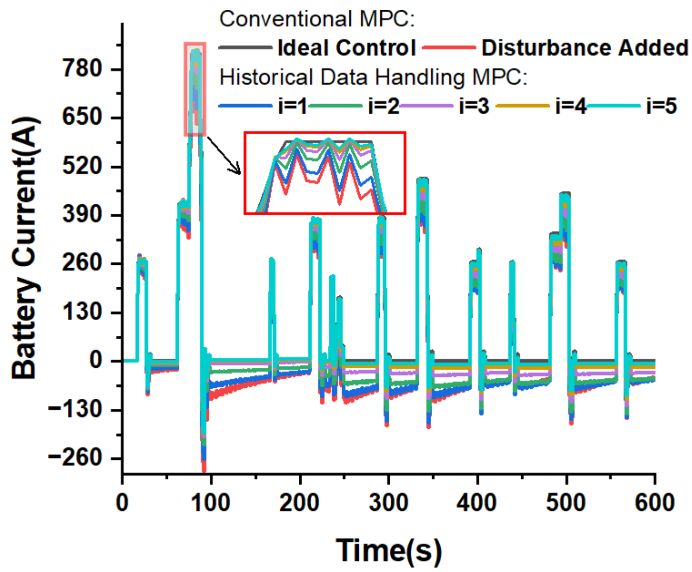

Fig. 5. Battery Current

Tables I summarize the reduction in battery current and supercapacitor voltage errors over multiple iterations. The MAE and MAPE calculations in this table only consider data when the vehicle is in motion. Data from when the vehicle is stopped is excluded, as its calculation results are meaningless. Initially, both battery current and voltage errors are relatively high, with significant mean absolute error (MAE) and mean absolute percentage error (MAPE) values, reflecting the impact of disturbances.

As the iteration progresses, these errors decrease substantially. By the fifth iteration, both battery current and voltage errors have reduced significantly compared with the conventional MPC and the first iteration, with lower MAE and MAPE values indicating improved accuracy. The MAPE of battery current decrease from 9.37% to 5.62% and the MAPE of supercapacitor voltage decrease from 0.467% to 0.092%. This progressive reduction indicates the convergence of the control strategy, which effectively dampens the fluctuations and stabilizes the battery current and supercapacitor voltage. Although MAPE of battery current is still higher than 5%, it's much smaller than the first iteration.

This result demonstrates the convergence and robustness of the control algorithm. The continual error reduction highlights the control strategy's effectiveness in minimizing fluctuations,

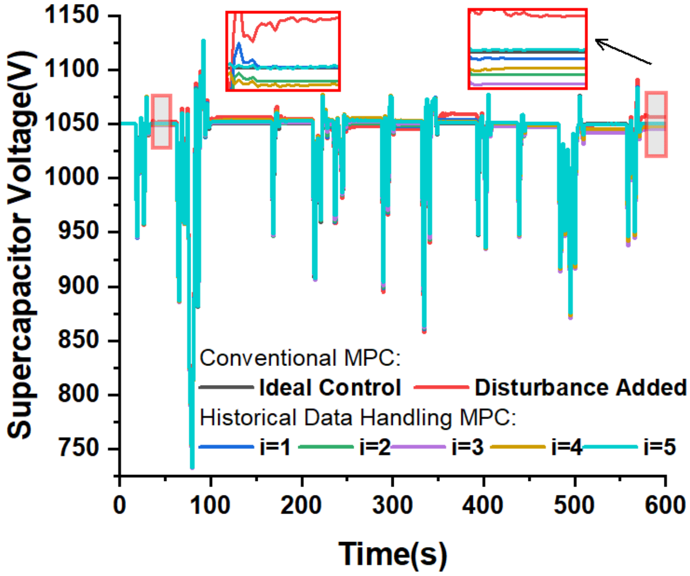

Fig. 6. Supercapacitor Voltage

stabilizing battery current and supercapacitor voltage, enhancing energy efficiency, reducing battery stress, and ensuring a stable power supply and voltage stability from the supercapacitor.

TABLE I

Control Iterations	Battery Current		Supercapacitor Voltage	
	MAE	MAPE (%)	MAE	MAPE (%)
1	20.87	9.37	4.73	0.467
2	13.44	8.14	3.52	0.332
3	10.53	7.25	2.60	0.280
4	9.81	6.09	1.72	0.166
5	8.76	5.62	0.88	0.092

VI. Conclusion

This article designs an electric vehicle energy management system based on MPC, including MPC formulation and implementation. The convex hull of historical data is used as a constraint for model predictive control, which improves the control performance of real-time control under disturbance and uncertainty. This energy management system is suitable for electric vehicle driving scenarios with repeated routes, such as buses.

This research illustrates the effectiveness of the proposed historical data handling MPC algorithm. The iterative reduction in errors for both battery current and supercapacitor voltage indicates a well-functioning control system that adapts to disturbances and optimizes energy management in real time. This performance improvement can be achieved within 5 iterations, which highlights the robustness and adaptability of the control strategy, making it highly suitable for applications in electric vehicles operating under variable load conditions.

Acknowledgment

The author affirms that the submitted work is original and that proper credit has been given for any references to others' work.

References

[1] C. Cunanan, M.-K. Tran, Y. Lee, S. Kwok, V. Leung, and M. Fowler, "A review of heavy-duty vehicle powertrain technologies: Diesel engine vehicles, battery electric vehicles, and hydrogen fuel cell electric vehicles," *Clean Technologies*, vol. 3, no. 2, pp. 474–489, 2021.

[2] M. Zandi, A. Payman, J.-P. Martin, S. Pierfederici, B. Davat, and F. Meibody-Tabar, "Energy management of a fuel cell/supercapacitor/battery power source for electric vehicular applications," *IEEE Transactions on Vehicular Technology*, vol. 60, no. 2, pp. 433–443, 2011.

[3] A. Etxeberria, I. Vechiu, H. Camblong, and J.-M. Vinassa, "Hybrid energy storage systems for renewable energy sources integration in microgrids: A review," in *2010 Conference Proceedings IPEC*. IEEE, 2010, pp. 532–537.

[4] A. S. Mohammed, S. M. Atnaw, A. O. Salau, and J. N. Eneh, "Review of optimal sizing and power management strategies for fuel cell/battery/super capacitor hybrid electric vehicles," *Energy Reports*, vol. 9, pp. 2213–2228, 2023.

[5] M. Kisacikoglu, M. Uzunoglu, and M. Alam, "Fuzzy logic control of a fuel cell/battery/ultra-capacitor hybrid vehicular power system," in *2007 IEEE vehicle power and propulsion conference*. IEEE, 2007, pp. 591–596.

[6] B. Hredzak, V. G. Agelidis, and G. Demetriades, "Application of explicit model predictive control to a hybrid battery-ultracapacitor power source," *Journal of Power Sources*, vol. 277, pp. 84–94, 2015.

[7] Z. S. Yu *et al.*, "Vehicle theory," *China Machinery Industry Press, Beijing*, 2000.

[8] Vehicle and fuel emissions testing. EPA. [Online]. Available: https://www.epa.gov/vehicle-and-fuel-emissions-testing/dynamometer-drive-schedules

[9] Z. Song, H. Hofmann, J. Li, J. Hou, X. Han, and M. Ouyang, "Energy management strategies comparison for electric vehicles with hybrid energy storage system," *Applied Energy*, vol. 134, pp. 321–331, 2014.

[10] P. Golchoubian and N. L. Azad, "Real-time nonlinear model predictive control of a battery–supercapacitor hybrid energy storage system in electric vehicles," *IEEE Transactions on Vehicular Technology*, vol. 66, no. 11, pp. 9678–9688, 2017.

[11] S. Ermon, Y. Xue, C. Gomes, and B. Selman, "Learning policies for battery usage optimization in electric vehicles," *Machine learning*, vol. 92, pp. 177–194, 2013.

[12] Y. Zhou, K. Gao, D. Li, Z. Xu, and F. Gao, "Data-efficient constrained learning for optimal tracking of batch processes," *Industrial & Engineering Chemistry Research*, vol. 60, no. 43, pp. 15 658–15 668, 2021.